

Structural Phase Transition of Vanadium at 69 GPa

Yang Ding,^{1,*} Rajeev Ahuja,² Jinfu Shu,³ Paul Chow,¹ Wei Luo,² and Ho-kwang Mao^{1,3}

¹*HPCAT, Geophysical Laboratory, Carnegie Institution of Washington, Building 434E, 9700 South Cass Avenue, Argonne, Illinois 60439, USA*

²*Department of Physics, Condensed Matter Theory Group, Box 530, Uppsala University, SE-751 21 Uppsala, Sweden*

³*Geophysical Laboratory, Carnegie Institution of Washington, 5251 Broad Branch Road NW, Washington, DC 20015, USA*

(Received 17 June 2006; revised manuscript received 11 October 2006; published 22 February 2007)

A phase transition was observed at 63–69 GPa and room temperature in vanadium with synchrotron x-ray diffraction. The transition is characterized as a rhombohedral lattice distortion of the body-centered-cubic vanadium without a discontinuity in the pressure-volume data, thus representing a novel type of transition that has never been observed in elements. Instead of driven by the conventional *s-d* electronic transition mechanism, the phase transition could be associated with the softening of C_{44} trigonal elasticity tensor that originates from the combination of Fermi surface nesting, band Jahn-Teller distortion, and electronic topological transition.

DOI: [10.1103/PhysRevLett.98.085502](https://doi.org/10.1103/PhysRevLett.98.085502)

PACS numbers: 62.50.+p, 31.15.Ar, 61.50.Ks, 63.20.Pw

Elucidating the structural stability trends and the underlying mechanisms in elemental metals is a fundamental topic in condensed matter physics. Of particular interest are the transition metals that exhibit the hcp (hexagonal close packed)-bcc (body centered cubic)-hcp-fcc (face centered cubic) sequence of structures with increasing either atomic number or pressure. The driving force behind such structural variations is typically attributed to the increasing *d*-band filling with increasing atomic numbers [1–3] or the pressure-induced *s-d* electronic transitions [4,5]. According to the structural sequence, the vanadium group metals (V, Nb, and Ta) are commonly predicted to be stable in the bcc structure up to at least a couple of hundred GPa [1–5]. As no structural change has been reported so far [6], they now become standard examples demonstrating the success of applying first principles calculations for structural stability of elemental metals. However, the latest lattice dynamics calculations, aimed at understanding the T_c anomaly in vanadium around 120 GPa [7], suggested a possible shear instability due to phonon softening in vanadium [8,9]. This prediction prompted our interest to reinvestigate the structural transition of vanadium under high pressure.

Using diamond-anvil cell and synchrotron x-ray diffraction techniques, we report in this Letter for the first time the observation of a transition from bcc to a rhombohedral phase in vanadium at 69 GPa. The vanadium sample displays the characteristics of a second-order phase transition across which the pressure dependences of lattice parameters are continuous, but their slopes are discontinuous. This form of transition has never been reported in any transition metal or other pure element, and represents an entirely different trend from previous reports. Moreover, the discovery reveals that electronic structure features other than the *s-d* transition, such as Fermi surface nesting and electronic topological transition, could be the origin of struc-

ture variations, and provides essential information for proper reevaluation of the T_c anomaly at 120 GPa which occurs in the new phase rather than the simple bcc vanadium.

A Mao-type symmetric diamond-anvil cell with two beveled diamond anvils (80 μm central flat beveled at 8° angle from the 400 μm culet) was used to preindent the Re gasket from the original thickness of 250 μm to 20 μm central thickness. A 50 μm diameter hole was drilled at the center of the gasket to form the sample chamber. Powder vanadium sample (purity 99.99% from Alfa Aesar) was loaded in the sample chamber without a pressure medium. A 3–5 μm platinum powder chip used as the pressure standard was added to a quadrant of the sample area. High-pressure angle-dispersive diffraction experiments were performed at 16ID-B station of the HPCAT Sector, Advanced Photon Source, Argonne National Laboratory. The monochromatic x-ray beam, operated at 29.21 and 30.87 keV, was focused to $\sim 20 \mu\text{m}$ in diameter at the sample position. The small beam was used to select specific sample areas. Areas that only contained pure vanadium diffraction pattern (e.g., Fig. 1) were used for clear identification of phase transition without possible complications from the Pt and Re diffraction, and areas that contained both vanadium and Pt were used for pressure determination and confirmation of the vanadium diffraction. Pressure was determined from the equation of state of platinum [10,11] based on three diffraction lines: 111, 200, and 220. The uncertainty in *d*-spacing measurements was estimated to be less than 0.007 Å, which corresponded to 4–5 GPa uncertainty around 100 GPa. The diffraction patterns were collected using a MAR345 image plate (pixel size $100 \times 100 \mu\text{m}^2$), and the exposure time was typically 30–600 s. The two-dimensional diffraction rings on the image plate (Fig. 1) were integrated with the FIT2D program [12] to produce diffraction patterns of intensity

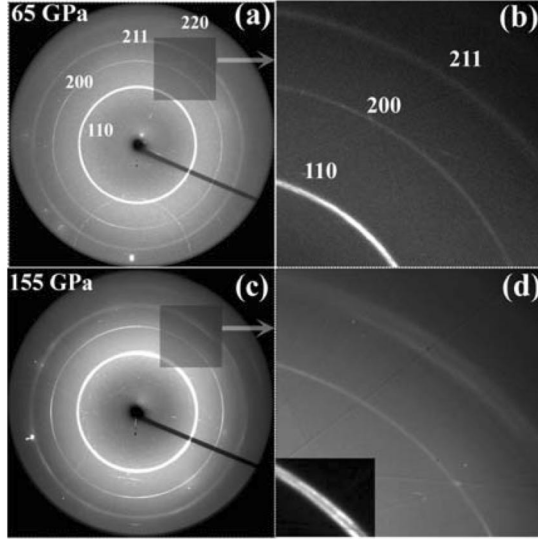


FIG. 1. (a) The diffraction pattern of vanadium recorded on an image plate at 65 GPa under nonhydrostatic conditions. The indexing is based on a bcc lattice. (b) The enlarged image of the shadowed area in (a). (c) The diffraction pattern of vanadium at 155 GPa. (d) The enlarged image of the shadow area in (c).

versus 2θ (Fig. 2), and the lattice parameters were obtained from the refinement of diffraction patterns with the GSAS program [13].

Experiments were carried out up to 155 GPa. Vanadium remained in the bcc structure until the 110 and 220 peaks split above 65 GPa, whereas the 200 diffraction stayed as a single sharp line up to the maximum pressure (Fig. 1). The changes evinced a transition from cubic to a rhombohedral lattice due to the elongation or contraction of a unit-cell body diagonal [111] relative to the other three body diagonals, similar to the B2-R phase transformation discovered in NiTi alloys [14]. Figure 2 shows the diffraction patterns of vanadium at 65, 90, and 155 GPa. The transformation from the bcc structure ($Im\bar{3}m$) into a rhombohedral structure ($R\bar{3}m$) is illustrated by the insets in Fig. 2(b). The cubic unit cell with lattice parameter a_c can also be represented by a rhombohedral unit cell with lattice parameter a_R and α ; the two unit cells are related by $a_R = \frac{\sqrt{3}}{2}a_c$ and $\alpha = 109.47^\circ$. When α deviated from 109.47° , the symmetry was reduced from cubic to rhombohedral. The cubic 110 diffraction peak was no longer degenerate but split into rhombohedral $0\bar{1}1$ and 100 , and the cubic 211 split into rhombohedral $2\bar{1}0$, $2\bar{1}\bar{1}$, and 110 . The rhombohedral α angle could thus be calculated from the splitting of the cubic 110 and 211 diffraction lines as shown in the insets in Fig. 2(c).

In order to eliminate the possibility of anisotropic broadening due to strong uniaxial stress [15], we performed an additional quasihydrostatic experiment to 76 GPa on vanadium powder sample using helium as pressure transmission medium [16]. As shown in Fig. 3 in the quasihydrostatic experiment above the transition pressure, the 110, 211, and

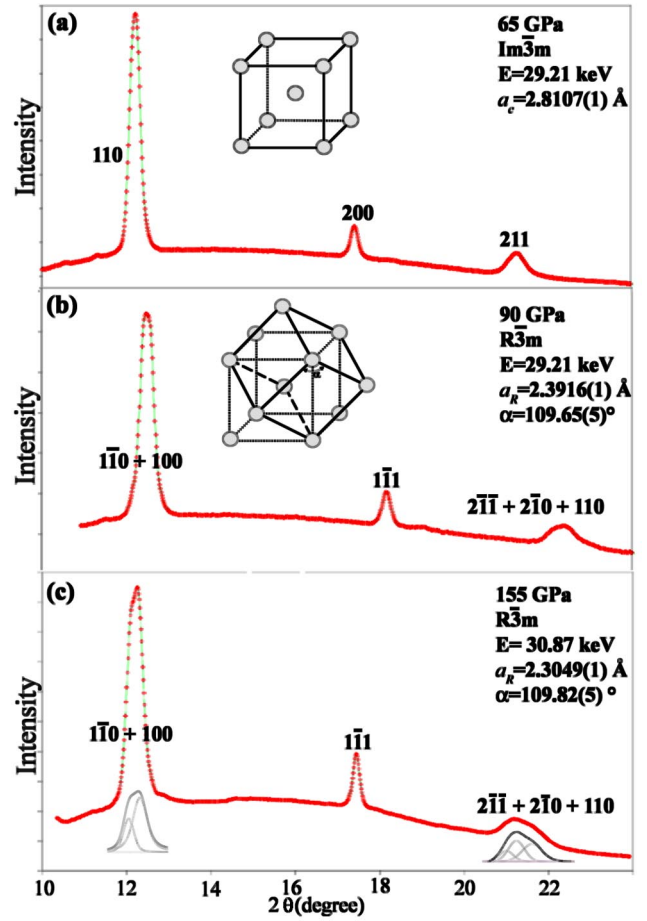


FIG. 2 (color online). Nonhydrostatic x-ray diffraction patterns of vanadium at (a) 65 GPa, (b) 90 GPa, and (c) 155 GPa. The inset in (b) demonstrates the transformation of vanadium from cubic to the rhombohedral structure. The insets in (c) demonstrate the resolved splitting peaks according to refinement of rhombohedral structure model. E denotes the energy of x-ray photon used for diffraction.

220 reflections also split, whereas 200 remained as a single sharp peak, thus unambiguously confirming the phase transition from cubic to rhombohedral lattice.

Takemura studied x-ray diffraction of vanadium up to 154 GPa [6]. Although he did not claim any structural transition, the diffraction pattern of vanadium in his report at 154 GPa indeed showed a very broad 110 peak, a shoulder on the low angle side, and a sharp 200 peak that are consistent with the present conclusion of a bcc-rhombohedral transition.

The phase transition displayed a lattice distortion without a discontinuity in the pressure-volume plot [Fig. 4(a)], thus characterizing a second-order displacive phase transition. For example, for the nonhydrostatic series, the deviation of α from 109.47° (cubic) at 65 GPa to 109.65° at 90 GPa, and to 109.82° at 155 GPa provides a direct measurement of symmetry breaking strain. The transition pressure was analyzed based on Landau theory, in which the order parameter $\langle Q \rangle$ was defined as $(\alpha/\alpha_0) - 1$,

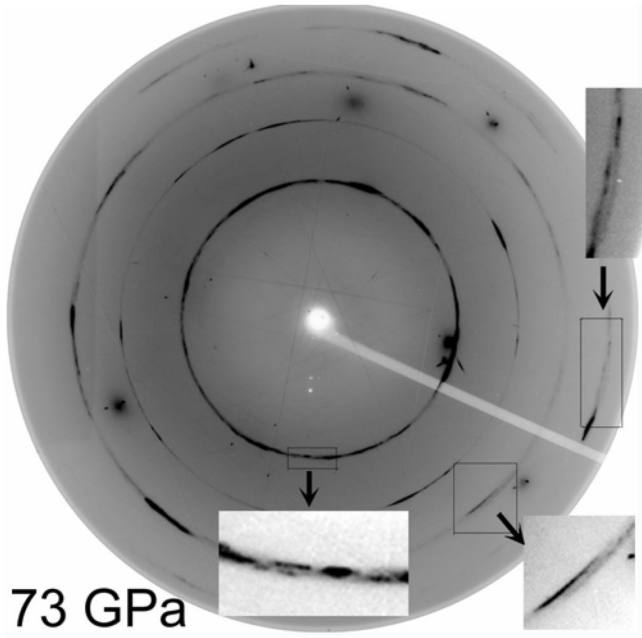


FIG. 3. The diffraction pattern of vanadium at 73 GPa under quasihydrostatic conditions recorded on an image plate. The diffraction rings are spotty because the sample grinding was minimized in order to avoid the introduction of residual strain. From inside outward, the four rings are originally 110, 200, 211, and 220 reflections of the cubic phase. Insets are zoomed images showing the splitting of 110, 211, and 220 rings after rhombohedral transition.

where α_0 is 109.47° for the cubic phase. $\langle Q \rangle^2$ is proportional to spontaneous lattice strain [17]. The transition pressures P_c , obtained by fitting the equation $\langle Q \rangle = C(P - P_c)^{1/2}$, where C is a constant, are determined to be 69(1) GPa for nonhydrostatic and 63(1) GPa for quasihydrostatic experiments [Fig. 4(b)]. The bulk moduli obtained from nonhydrostatic and quasihydrostatic experiments are $K_0 = 195(3)$ GPa with $K'_0 = 3.5(2)$ and $K_0 = 158(1)$ GPa with $K'_0 = 3.9(2)$ [Fig. 4(a)], respectively, by fitting the 3rd order Birch-Murnaghan equation of the state to the pressure-volume data of bcc vanadium [Fig. 4(a)]. The quasihydrostatic results in our experiments agree well with $K_0 = 162(5)$ GPa and $K'_0 = 3.5(5)$ from quasihydrostatic experiments by Takermura [6]. Our nonhydrostatic data points shift to slightly higher pressure side of the quasihydrostatic data points; this agrees with the well documented effect of nonhydrostaticity in high-pressure literatures (for example, Ref. [18]).

It is known that vanadium group metals display Kohn anomalies [19,20] in the transverse acoustic phonon branch along the $[\xi 00]$ direction, and the anomaly at $\xi = 1/4$ was predicted to soften under high pressure and eventually become imaginary at 130 GPa [8] (but the mechanism of softening was not discussed by the authors). This mode is related to the shear elasticity tensor by $C_{44} = \omega^2 \rho / K^2$, where ω , ρ , and K are phonon frequency, density, and phonon wave vector, in the long wavelength limit, and C_{44}

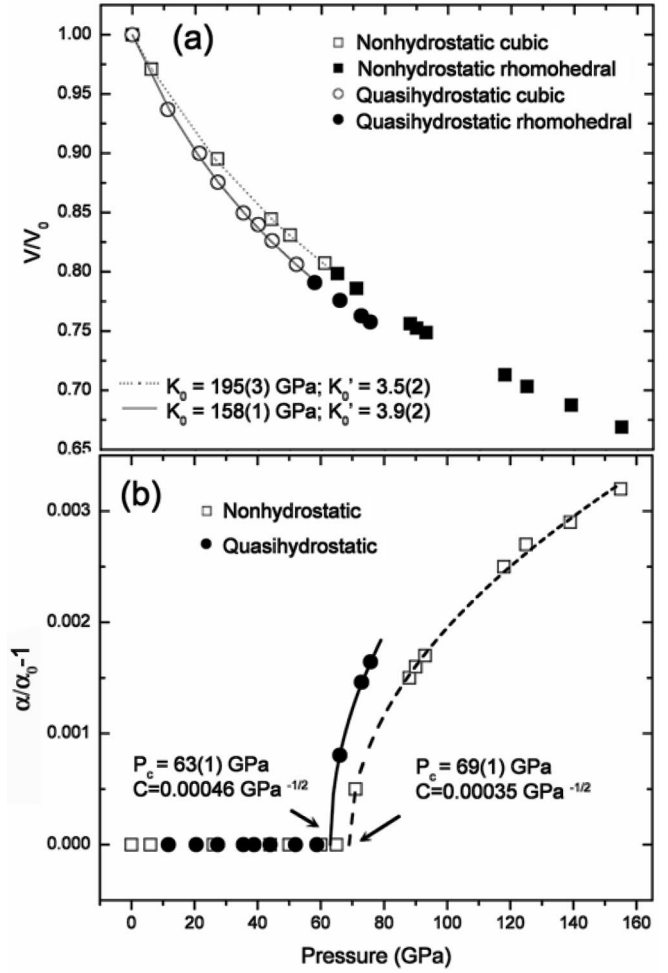


FIG. 4. (a) The pressure-volume data of vanadium. The lines represent the fitted results using 3rd order Birch-Murnaghan equation of state. (b) The plot of order parameter $\langle Q \rangle$, defined as $(\alpha/\alpha_0) - 1$ where $\alpha_0 = 109.47^\circ$, vs pressure. The phase transition pressures determined from nonhydrostatic and quasi-hydrostatic experiments are 69(1) GPa and 63(1) GPa, respectively, using equation $\langle Q \rangle = C(P - P_c)^{1/2}$.

is associated with a trigonal distortion of the cubic lattice. Consequently, the pressure-induced rhombohedral transition in vanadium could be triggered by the C_{44} instability due to the phonon softening.

The d -band filling via s - d transition is typically regarded as a major driving force behind the pressure-induced structure transitions in transition metals. However, it is unlikely that the C_{44} softening in vanadium is driven by s - d transition. For instance, chromium ($3d^5 4s^1$) with two more electrons in the d band than vanadium ($3d^3 4s^2$) shows no softening but stiffening of C_{44} (C_{44} of vanadium is 43 GPa [21], while that of chromium is 100 GPa [22]). Therefore, other mechanisms must be considered.

Very recent *ab initio* calculations on bcc vanadium by Landa *et al.*, employing full-potential linear muffin-tin orbitals (FPLMTO) [23] and exact muffin-tin orbital calculations (EMTO) [9] methods, show that C_{44} reaches a maximum and softens at pressures above 60 GPa and drops

to zero at 120 (FPLMTO) to 180 GPa(EMTO). According to these calculations [9,23], the Kohn anomaly at $\xi = 1/4$ along $[\xi 00]$ in the transverse acoustic phonon mode was a consequence of Fermi surface nesting in the third band. Upon compression, the nesting vector $q_n = 0.48\pi/\alpha$ decreased and the effect of the Kohn anomaly on C_{44} increased. When q_n became zero, a minimum appeared in the shear elastic constant C_{44} due to an electronic topological transition in third band. Meanwhile, the pressure-induced s - d transition also introduced band Jahn-Teller effects on C_{44} softening, but this effect was secondary to those of Fermi surface nesting and electronic topological transition [9]. The physical meaning of the predicted trigonal elasticity tensor C_{44} instability at 120–180 GPa is an upper limit, above which a finite shear would lead to infinitely large strain in the bcc vanadium and cause the collapse of the structure; a phase transition must occur before reaching this limit. Our experimental observation of the rhombohedral transition at 63–69 GPa is consistent with the predicted upper limit.

In summary, a phase transition of vanadium from bcc to a rhombohedral structure was observed at 63–69 GPa, as indicated by the splitting of diffraction lines 110 and 211 of the bcc vanadium. The transition displayed second-order characteristics, without discontinuity in the pressure-volume curve. The transition could be associated with a soft-mode phonon induced C_{44} instability that originates from the Fermi surface nesting. The occurrence of the rhombohedral structure in vanadium indicated that electronic structure features other than s - d transition, such as Fermi surface nesting, electronic transitions, and band Jahn-Teller effects could be also important driving forces to induce the structure transitions and in turn result in the deviations from the hcp-bcc-hcp-fcc structural sequence. In addition, the bcc-rhombohedral transition in vanadium provides essential information for proper reevaluation of the T_c anomaly at 120 GPa.

We are grateful to Y. Meng, S. V. Sinogeikin, and H. Liu for the help on the beam line, and we are also thankful for the valuable comments and suggestions from anonymous reviewers. This work was performed at HPCAT (Sector 16), Advanced Photon Source (APS), Argonne National Laboratory. Use of the HPCAT facility was supported by DOE-BES, DOE-NNSA (CDAC), NSF, DOD-TACOM, and the W.M. Keck Foundation. Use of the APS was supported by DOE-BES, under Contract No. W-31-109-ENG-38.

*Corresponding author.

Email address: yding@hpcat.aps.anl.gov

- [1] J. Duthie and D. Pettifor, Phys. Rev. Lett. **38**, 564 (1977).
- [2] H. L. Skriver, Phys. Rev. B **31**, 1909 (1985).
- [3] J. A. Moriarty, Phys. Rev. B **45**, 2004 (1992).

- [4] A. K. McMahan, Physica (Amsterdam) **B139–140**, 31 (1986).
- [5] G. B. Grad, P. Blaha, J. Luitz, K. Schwarz, A. Fernández Guillermot, and S. J. Sferco, Phys. Rev. B **62**, 12 743 (2000).
- [6] K. Takemura, 2000 *Proceedings of the International Conference on High Pressure Science and Technology, AIRAPT-17 (Honolulu, July 1999)*, edited by M. H. Manghnani, W. J. Nellis, and M. F. Nicol (University Press, India, 2000), p. 443.
- [7] M. Ishizuka, M. Iketani, and S. Endo, Phys. Rev. B **61**, R3823 (2000).
- [8] N. Suzuki and M. Otani, J. Phys. Condens. Matter **14**, 10 869 (2002).
- [9] A. Landa, J. Klepeis, P. Söderlind, I. Naumov, L. Vitos, and A. Ruban, J. Phys. Condens. Matter **18**, 5079 (2006).
- [10] N. C. Holmes, J. A. Moriarty, G. R. Gathers, and W. J. Nellis, J. Appl. Phys. **66**, 2962 (1989).
- [11] H. Cynn and C. S. Yoo, Phys. Rev. B **59**, 8526 (1999).
- [12] A. P. Hammersley, S. O. Svensson, M. Hanfland, A. N. Fitch, and D. Häusermann, High Press. Res. **14**, 235 (1996).
- [13] A. C. Larson and R. B. Von Dreele, General Structure Analysis System (GSAS), Los Alamos National Laboratory Report No. LAUR, 1994, pp. 86–748.
- [14] J. Khalil-Allafi, W. W. Schmahl, and T. Reinecke, Smart Materials and Structures **14**, S192 (2005).
- [15] N. Funamori, M. Funamori, R. Jeanloz, and N. Hamaya, J. Appl. Phys. **82**, 142 (1997), and references therein.
- [16] Hydrostatic compression experiment with helium as a transmission medium was conducted on vanadium powder from the same batch as used in nonhydrostatic experiments. A compacted vanadium powder chip of $30 \times 30 \times 10 \mu\text{m}$ was loaded together with ruby and platinum pressure standards in a Mao-type symmetric diamond-anvil cell, and the vanadium sample was well separated from Pt pressure standard. Two beveled diamond anvils ($200 \mu\text{m}$ flat beveled from a $400 \mu\text{m}$ culet at an angle of 8°) were used with a $90 \mu\text{m}$ hole on a $30 \mu\text{m}$ thick, preindented rhenium gasket. The diffraction experiments were performed at the 16ID-B station of HPCAT with a $5 \times 7 \mu\text{m}^2$ monochromatic x-ray beam operated at 30.57 keV. The sample and Pt diffraction peaks remain sharp, and the ruby fluorescence peaks remain well resolved, indicating hydrostatic condition.
- [17] K. Aizu, J. Phys. Soc. Jpn. **28**, 706 (1970).
- [18] T. S. Duffy, G. Y. Shen, D. L. Heinz, J. F. Shu, Y. Z. Ma, H. K. Mao, R. J. Hemley, and A. K. Singh, Phys. Rev. B **60**, 15 063 (1999).
- [19] Y. Nakagawa and A. D. B. Woods, Phys. Rev. Lett. **11**, 271 (1963).
- [20] M. W. Finnis and K. L. Kear, Phys. Rev. Lett. **52**, 291 (1984).
- [21] D. I. Bolef, J. Appl. Phys. **32**, 100 (1961).
- [22] D. I. Bolef and J. de Klerk, Phys. Rev. **129**, 1063 (1963).
- [23] A. Landa, J. Klepeis, P. Söderlind, I. Naumov, O. Velikokhatnyi, L. Vitos, and A. Ruban, J. Phys. Chem. Solids, **67**, 2056 (2006); J. Klepeis and P. Söderlind, Bull. Am. Phys. Soc. **49**, 496 (2004).